

Reachability Guarantees for Energy Arbitrage

Tomás Tapia and Yury Dvorkin

Abstract—This paper introduces a unified framework for battery energy arbitrage under uncertain market prices that integrates chance-constrained terminal state-of-charge requirements with online threshold policies. We first cast the multi-interval arbitrage problem as a stochastic dynamic program enhanced by a probabilistic end-of-horizon state-of-charge (SoC) constraint, ensuring with high confidence that the battery terminates within a prescribed energy band. We then apply a k -search algorithm to derive explicit charging (buying) and discharging (selling) thresholds with provable worst-case competitive ratio, and compute the corresponding action probabilities over the decision horizon. To compute exact distributions under operational limits, we develop a probability redistribution pruning method and use it to quantify the likelihood of meeting the terminal SoC band. Leveraging the resulting SoC distribution, we estimate the minimum stopping-time required to satisfy the SoC chance constraint. Computational experiments on historical real price data demonstrate that the proposed framework substantially improves the estimation of SoC evolution and supports chance-constraint satisfaction.

I. INTRODUCTION

MULTI-period optimization is indispensable for the efficient operation of energy-constrained resources, such as battery storage, which are characterized by complex intertemporal state-of-charge (SoC) dynamics and operational limits. For both asset- and system-level perspectives, decision-making processes must rigorously account for economic trade-offs, which are inherently influenced by operational variability, uncertainty, and risk tolerance, as well as for the need to reconcile asset- and system-level objectives.

From an asset perspective, in terms of energy arbitrage, battery units must determine optimal charge and discharge decisions in response to both instantaneous and forecast price signals. This task leads to a high-dimensional decision space, where multiple admissible SoC trajectories may lead to the identical SoC level at the end-of-horizon, but be differently aligned with desired system-level performance. From a system perspective, the finite energy capacity of storage resources, exacerbated by inter-temporal limits, may necessitate overly conservative operational decisions due to under-utilization of storage capacity. In addition, inevitable variability and errors of the renewable generation, load, and price forecasts commonly result in adjustments to solutions of the decision-making routines, referred to below as *replanning* point.

While battery storage is technically well positioned to respond to variability and forecast errors, in practice both real-time (RT) and day-ahead (DA) market software typically rely on deterministic forecasts without hedging mechanisms for volatility [1]. As a result, batteries may overdischarge early in response to unexpected price spikes, leaving inadequate SoC for later periods when the grid is also likely to experience tight supply conditions, high demand, or reliability risk (referred to as *critical hours*). Notably, in addition to lacking sufficient energy during critical hours, batteries may also overcharge beyond optimal levels, reducing system operational flexibility

and increasing congestion risks, or stop charging and discharging prematurely, creating power shortages.

System operators have explored different mechanisms in preparation to critical hours risks imposed by large adoption rates of grid-scale batteries via managing SoC requirements. California Independent System Operator (CAISO) introduced a Minimum State-of-Charge (MSOC) program in 2022. This mechanism was not integrated into the market-clearing routine and functioned as an administrative overlay on the DA market, requiring certain batteries to reserve a fraction of their energy to remain available during peak-demand and evening ramp periods [2]. Although MSOC expired in 2023 and was not extended due to operational improvements in forecast processes and bidding behavior, this rule was viewed as a short-term measure to maintain grid reliability with some economic and efficiency limitations [3]. However, its underlying objective can still be replicated through improved exceptional dispatch, which compensates batteries for missed market opportunities and incentivizes energy retention during high-value intervals. Similarly in 2022, the Electric Reliability Council of Texas (ERCOT) approved the Nodal Protocol Revision Request 1186 (NPRR1186). This protocol introduces changes to track and monitor SoC, ensuring compliance with ancillary service requirements, and obligations for a minimum SoC level so that system operators can estimate deliverability for the whole committed period [4]. However, MSOC and NRR1186 are administrative mechanisms that operate outside the market-clearing process and are thus prone to the limitations of ad hoc out-of-market interventions [5].

We propose a framework to reconcile the system and asset perspective by quantifying the probability of remaining within a secure terminal SoC band. This framework employs a competitive threshold policy motivated by policy requirements aimed at ensuring the deliverability of energy arbitrage, regulation and reserve services. This approach enables us to determine the battery’s *stopping time*, the point at which it must start preserving energy to avoid violating terminal SoC constraints, and the associated cost of stopping. This framework provides system operators with sufficient advance notice to take corrective actions and re-dispatch the system.

We illustrate the main idea behind the proposed framework using Fig. 1, which displays the evolution of the SoC (e_t) for a given battery storage asset through a finite time horizon T . Value e_0 corresponds to the initial SoC, and value e^{target} is the SoC end-of-horizon target (e.g., as determined by the DA schedule or by other means), while δ is a user-defined tolerance margin (e.g., set by the system policy). Together, the red bracket at T highlights the required final SoC band $\mathcal{E} = [e^{\text{target}} \pm \delta]$. The solid blue line represents the realized SoC trajectory e_t up to some *replanning* time τ , with red blocks indicating the accumulated error from the original schedule. After τ , the blue line represents the DA-planned SoC trajectory aiming to reach the final SoC band. At time τ ,

each decision $a_t \in \{-1, 0, +1\}$ (discharge, idle, or charge) generates three branches (black arrows) in a decision tree, capturing all possible future trajectories. Finally, the orange dotted lines indicate the minimum E_{\min} and maximum E_{\max} SoC capacity limits, respectively. Thus, we develop an approach that finds time τ^* and the replanning trajectory (show by the green arrows in Fig. 1) that assure the required final SoC band (\mathcal{E}) with a given probability. To this end, we develop an approach to optimize the stopping time criterion to begin preserving energy to meet a given end-of-horizon SoC band target. We also provide an explicit performance guarantee that quantifies the probability that the battery will remain within a target SoC band under uncertain price trajectories.

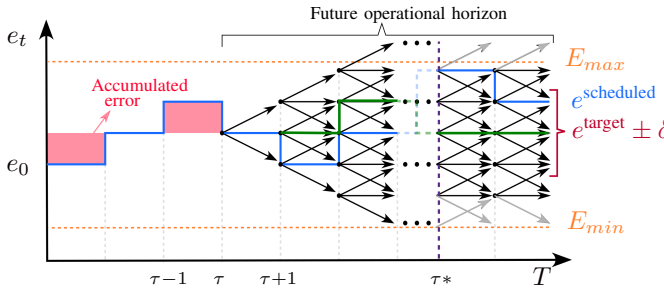


Fig. 1: State-of-charge and action trajectories for the battery arbitrage problem.

A. Literature review

In the past decade, optimization techniques for SoC and battery storage management have advanced rapidly [6], and [7] presents a comprehensive survey of such techniques and details future research challenges. Related to this paper, one of the major challenges is estimating the value of stored energy in energy arbitrage applications. In this context, [8] estimates the historical annual value of stored energy for a price-taking energy storage system performing arbitrage in the PJM market, considering factors such as fuel prices, transmission line constraints, battery efficiency, capacity limits, etc. Similarly, [9] estimates the value of stored energy in the National Electricity Market considering arbitrage opportunities and capacity service provision. Bolun et al. [10] present an analytical formulation for the operational value of energy storage for a price-taker battery asset under multistage uncertainty.

Beyond the valuation of stored energy, recent studies have focused on analyzing the profitability of energy storage through different market structures. For instance, [11] analyzes the profitability of battery storage investments, including an arbitrage analysis to determine the optimal location and sizing of energy storage systems. The authors in [12] propose a strategic framework for energy arbitrage and evaluates performance of different energy storage technologies, accounting for variations in overall efficiency and life-cycle costs, and [13] introduces alternative SoC market models and examines arbitrage opportunities in different price settings.

The authors in [14] examine energy arbitrage opportunities for grid-level battery storage in the DA market, allowing corrective actions in the RT market. Similarly, [15] proposes an analytical stochastic dynamic programming (SDP) algorithm to optimize variable-efficiency energy storage for

price arbitrage in the RT market. The authors in [16] analyze the integration of battery storage in DA security-constrained unit-commitment, while [17], [18] present chance-constrained pricing models for energy storage systems. Furthermore, the authors in [19] introduce a cooperative DA dispatch framework in which energy storage provides multiple regulation services to improve system reliability, and [20] introduces a nested Markov decision process model that co-optimizes energy storage for joint energy arbitrage and frequency regulation.

To cope with the impacts of forecast errors, a rich literature on online policies has emerged. Its foundation lies in classical threshold policies, such as the secretary problem [21], [22] and stopping time theory [22], [23]. Threshold policies, such as k -search, offer a simple method to determine a direct relationship between decisions and observed prices that could be exploited to estimate a stopping-time criterion while guaranteeing worst-case coverage. Recent works have extended online k -search methods specifically to the energy-storage arbitrage problem. Ref. [24] derives k -threshold purchase rules that guarantee a competitive ratio against a clairvoyant (perfect foresight) benchmark. The authors in [25] develop a unified online framework in which both buying and selling thresholds are dynamically adjusted based on the remaining action budget, while [12] analyzes arbitrage opportunities in different storage technologies and shows that simple threshold policies achieve near-optimal performance under realistic price distributions.

Recent machine learning driven approaches to inventory management and energy storage under price uncertainty increasingly emphasize reliable uncertainty quantification rather than point forecasting alone. Some works integrate learned forecasts into online policies [26] or thresholds to guide real-time decisions [27], while others incorporate switching costs into online optimization via threshold-based designs [28], [29]. A key recent direction is to couple decision-making with calibrated prediction sets as in [30], [31] to produce finite-sample prediction intervals for policy outcomes and to provide distribution coverage under data exchangeability assumptions. In our setting, conformal calibration provides coverage-guaranteed bounds for the terminal SoC as a distribution-free uncertainty layer. We empirically compare probability estimates based on assumed price distributions against conformalized quantile regression.

B. Contributions

The goal of this paper is to propose an operational framework that reconciles asset-level arbitrage decisions with system-level reliability requirements by quantifying the probability that a battery's SoC satisfies an end-of-horizon SoC target band constraint. Our contributions include:

- Extending the battery arbitrage problem by proposing a tractable framework to estimate the probability of a battery arriving within a prescribed terminal SoC target band at the end of the target horizon. The framework builds on the k -search method in [24] to incorporate the temporal evolution of worst-case price realizations and connect arbitrage decisions with terminal reachability.
- Introducing time dependent k -search thresholds that update with the remaining feasible charge/discharge actions,

conditioned by the current SoC level, capacity and rate limits. This design leverages available market forecast information to construct evolving worst-case maximum and minimum price sets and to adapt the decision thresholds accordingly. Using these thresholds, we define and price a stopping time that triggers a transition to an energy preservation mode required to satisfy the terminal chance constraint requirement.

- Validating the proposed probability estimates on real day-ahead price data by comparing (i) probability evaluations obtained under assumed price probability distributions and (ii) a distribution-free conformalized quantile regression (CQR) approach that constructs prediction set and provides empirical coverage for the terminal SoC.

II. ENERGY ARBITRAGE UNDER UNCERTAIN PRICE

Consider the battery arbitrage problem, where the battery asset aims to maximize its profits under energy price (λ_t) uncertainty, by charging (c_t) when the price is low, and discharging (d_t) when it is high, i.e., the profit is driven by the captured price difference. These decisions are made prior to observing the realization of λ_t and involve determining the future energy value. Thus, the battery arbitrage problem can be formulated as below:

$$\max_{e,c,d} \mathbb{E}_{\lambda} \left[\sum_{t=1}^T \lambda_t (d_t - c_t) \right] \quad (1a)$$

$$\text{s.t. } \left\{ \begin{array}{l} E_{\min} \leq e_t \leq E_{\max}, \\ e_t = e_{t-1} + a_t P, \end{array} \right. \quad (1b)$$

$$a_t = \begin{cases} 1, & \text{if charge} \\ -1, & \text{if discharge} \\ 0, & \text{if idle} \end{cases}, \quad (1c)$$

$$0 \leq c_t \leq P, \quad 0 \leq d_t \leq P, \quad \forall t \in \mathcal{T}, \quad (1d)$$

where (1a) corresponds to the objective function that aims to maximize energy arbitrage profit under uncertain energy price. Eq. (1b) denotes battery storage capacity limits. Eq. (1c) represents the battery dynamics, where $\eta < 1$ is used to denote charging and discharging efficiency. Finally, eq. (1d) represents the maximum charging and discharging limits.

As mentioned in [32], this problem can also be formulated as a dynamic optimization that incorporates additional penalty to enforce a given terminal SOC target band, e.g., e^{target} . Rather than imposing a penalty cost relative to e^{target} , the system operator could enforce a minimum requirement through a chance constraint. Specifically, at the terminal time T , where the SoC must stay within a tolerance band δ around e^{target} at minimum $(1-\epsilon)$ of the realizations. The chance constraint implementation is also suitable in this context because it allows for "soft" security margins that can be adjusted based on an user-defined tolerance to risk, which in turn allows balancing risk preferences and cost-based operational objectives. The chance constraint for the battery to achieve a prescribed SoC target band, given as $\mathcal{E} = [e^{\text{target}} \pm \delta]$, is defined:

$$\mathbb{P}_{\lambda} \{ e_T \in \mathcal{E} \} \geq 1 - \epsilon, \quad \forall T \in \mathcal{T}^{\text{target}}. \quad (2)$$

Since d_t and c_t are real variables, quantifying the future value of the energy stored is complex task due to the infinite number of possible combinations of the battery SoC. To address the

issue, we can consider a fixed rate for charging/discharging P , and consider perfect efficiencies $\eta = 1$. Let a_t represent the action at time t that replaces the variables c_t and d_t , taking the values: +1 for charging, -1 for discharging, and 0 for idle. Also, consider a single target time at $\mathcal{T}^{\text{target}} = \{T\}$. Given these assumptions, the problem in (1) is equivalent to:

$$\max_{a,e} \mathbb{E}_{\lambda} \left[\sum_{t=1}^T \lambda_t a_t P \right] \quad (3a)$$

$$\text{s.t. } E_{\min} \leq e_t \leq E_{\max} \\ e_t = e_{t-1} + a_t P, \quad \forall t \in \mathcal{T} \quad (3b)$$

$$a_t = \begin{cases} 1, & \text{if charge} \\ -1, & \text{if discharge} \\ 0, & \text{if idle} \end{cases}, \quad \forall t \in \mathcal{T} \quad (3c)$$

$$\mathbb{P}_{\lambda} \{ e_T \in \mathcal{E} \} \geq 1 - \epsilon, \quad (3d)$$

where the expression on (3a) corresponds to the maximization of the battery arbitrage profit considering constant charging and discharging power rates. Eq. (3b) corresponds to the battery dynamics that ensures that the change in SoC matches the action times the fixed rate. Eq. (3c) restricts control decisions to charging, discharging, or idling, and eq. (3d) is a chance constraint that ensures that the probability of ending within a given SoC band target exceeds a given probability level of $(1-\epsilon)$, where ϵ is an user-defined risk tolerance.

A. Price thresholds and probability transitions estimate

Threshold policies are decision rules based on predefined cut-off values and available information to support real-time decision-making. These mechanisms are particularly useful in inventory settings because of their interpretability, i.e., they can be implemented only using the current system state and each threshold has a direct operational meaning (e.g., in case of storage - charge, discharge or idle). Also, these mechanisms are aligned with energy arbitrage, which requires sequential decisions under uncertainty as market prices are revealed over time. These algorithms design a threshold function that defines a unique minimum (or maximum) acceptable value (or a sequence of such values) that a price that is being revealed must satisfy in order to charge, discharge, or idle. This threshold policy enables the determination of the price to take an action and, consequently, sets an economic value to the stopping criterion, i.e. when no action is taken.

In the context of battery arbitrage, the battery operator commits an energy schedule (i.e. a SoC trajectory) in the DA market. In real time, the battery actions may differ from this schedule, and the resulting deviation is settled at the realized RT price. Accordingly, it must decide whether to buy (charge), sell (discharge) or idle (stick to the DA SoC trajectory) using only the current observed RT price, without knowing future price realizations or deviations from the DA schedule. To prepare for uncertainty realizations, battery assets often quantify uncertainty by modeling uncertainty sets, generating scenarios, or estimating probability distributions. Fig. 2 shows a real-world example of a full-day price uncertainty set.

To evaluate performance of a given policy in the absence of probabilistic models, the *competitive ratio* is commonly used, which corresponds to the worst-case ratio between the

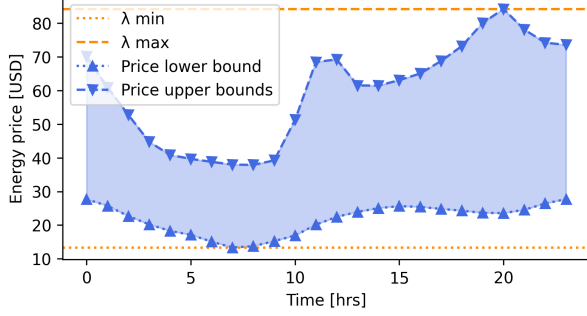


Fig. 2: Full-day price uncertainty set based on the PJM real-time prices data from 2011-2016. Dashed orange lines represent the minimum (λ^{\min}) and maximum (λ^{\max}) price values across the time horizon, while the dashed blue lines bound the possible realization for the energy price (λ_t).

outcome of an online algorithm policy $\text{ALG}_\pi(\lambda)$ and the offline optimum $\text{OPT}(\lambda)$ with perfect foresight. For instance, k -search algorithms are online methods that use threshold rules to make sequential decisions under uncertainty and have competitive guarantees. For a maximization problem, the competitive ratio $\alpha = \inf_\lambda \frac{\text{ALG}_\pi(\lambda)}{\text{OPT}(\lambda)}$. Equivalently, the policy π is α -competitive if $\text{ALG}_\pi(\lambda) \geq \frac{1}{\alpha} \text{OPT}(\lambda)$ for all λ , i.e., the online policy is guaranteed to achieve at least an α fraction of the offline optimum worst case. For a minimization problem, the definition is typically inverted [24].

When the values λ^{\min} and λ^{\max} are available, k -search algorithms leverage these bounds to construct a sequence of thresholds for *buy* and *sell* decisions. In a k -min search, the algorithm allows up to k_{ch} purchases at precomputed *buy* thresholds, whereas a k -max search allows up to k_{dis} sales when prices exceed *sell* thresholds. These thresholds are geometrically spaced across the price range to guarantee a provable competitive ratio relative to the offline optimal result, i.e., considering a perfect foresight [24].

Under the assumption that the number of possible discharge k_{dis} and charge k_{ch} actions are predefined, we can use the k -search algorithm to derive price thresholds to support the decision process. Thus, based on Algorithm 1 in [33] the j -th threshold to buy (charge) is defined as follows:

$$u_j^{\text{ch}} = \lambda^{\max} \left[1 - \left(1 - \frac{1}{\alpha} \right) \left(1 + \frac{1}{\alpha k_{\text{ch}}} \right)^{j-1} \right], \quad (4)$$

and i -th threshold to sell (discharge) energy corresponds to:

$$\ell_i^{\text{dis}} = \lambda^{\min} \left[1 + (\omega - 1) \left(1 + \frac{\omega}{k_{\text{dis}}} \right)^{i-1} \right], \quad (5)$$

where $j \in [1, k_{\text{dis}}]$ and $i \in [1, k_{\text{ch}}]$, and α and ω are the competitive ratios of the algorithm for discharging and charging energy, respectively. For instance, in the context of the k -max algorithm, the competitive ratio means that its performance is at most α times the performance of an optimal offline algorithm that has full knowledge of the future [24]. These thresholds do not consider battery capacity limits but, as we will show later, can be handled using explicit pruning and probability redistribution techniques.

In the worst-case scenario, k_{ch} and k_{dis} can be tuned to

achieve a desired trade-off between purchasing aggressiveness and sale conservatism. Thus, these threshold functions are a sequence of k_{ch} and k_{dis} thresholds $\{u_j^{\text{ch}}\}_{j=1}^{k_{\text{ch}}}$ and $\{\ell_i^{\text{dis}}\}_{i=1}^{k_{\text{dis}}}$, respectively, which is also called the reservation price policy. At each time t , the algorithm observes the revealed price λ_t and checks whether the number of charges executed is less than k_{ch} . If so, and if $\lambda_t \leq u_j^{\text{ch}}$ and $e_{t-1} + P \leq E_{\max}$, the battery charges energy. Otherwise, if the number of discharges executed is less than k_{dis} , $\lambda_t \geq \ell_i^{\text{dis}}$, and $e_{t-1} - P \geq E_{\min}$, the battery discharges energy. If neither condition is met, the battery remains idle. Whenever a revealed price *crosses* a threshold, triggering an action, but the corresponding capacity constraint is violated, the action is treated as idle and the associated threshold counter is not advanced.

Assume the battery operator has access to time-varying price bounds (e.g. probabilistic forecasts) over the remaining horizon (e.g. blue lines instead of orange lines in Fig. 2), namely $z^{\min}(t) = \{\lambda_\tau^{\min}\}_{\tau=t}^T$ and $z^{\max}(t) = \{\lambda_\tau^{\max}\}_{\tau=t}^T$. As time advances, these sets update because the remaining horizon shrinks, and the bounds z^{\min} and z^{\max} are time dependent. Let denote by $z^{\min}(t)$ the non-decreasing ordered list of the remaining lower bounds at time t , and by $z^{\max}(t)$ the non-increasing ordered list of the remaining upper bounds at time t . Then, we can adjust the j -th price threshold for the k -min algorithm to maintain the α -competitive guarantee as:

$$u_j^{\text{ch}}(t) = \frac{1}{\alpha k_{\text{ch}}} \left(\sum_{\hat{t}=1}^{t-1} \sum_{k=1}^{j-1} u_k^{\text{ch}}(\hat{t}) + \sum_{n=1}^{k_{\text{ch}}-(j-1)} z_n^{\max}(t) \right), \quad (6)$$

Similarly, we can modify the i -th price threshold for the k -max algorithm, maintaining the ω ratio:

$$\ell_i^{\text{dis}}(t) = \frac{\omega}{k_{\text{dis}}} \left(\sum_{\hat{t}=1}^{t-1} \sum_{k=1}^{i-1} \ell_k^{\text{dis}}(\hat{t}) + \sum_{n=1}^{k_{\text{dis}}-(i-1)} z_n^{\min}(t) \right). \quad (7)$$

Here, the first term corresponds to the previously activated price thresholds and actions taken. In particular, $u_k^{\text{ch}}(\hat{t})$ in (6) represents the charging threshold activated and $\ell_k^{\text{dis}}(\hat{t})$ in (7) represent the discharging thresholds activated at some time $\hat{t} < t$. The second term in the sum of (6) and (7) accounts for the remaining worst-case values in the lists $z^{\min}(t)$ and $z^{\max}(t)$. This structure adjusts the price threshold to avoid underestimating the worst-case realizations for charging or discharging decisions, because the bounds $[\lambda^{\min}, \lambda^{\max}]$ may correspond to price trajectories that are infeasible given the remaining time and SoC constraints. To consider only feasible decision trajectories at state (t, e_t) , we impose the following time and state dependent bounds:

$$\{z_n^{\min}(t)\}_{n=1}^{k_{\text{dis}}-(i-1)} \rightarrow \{z_n^{\min|\text{feas}}(t, e_t)\}_{n=1}^{K_{\min}^{\text{feas}}(t, e_t)}.$$

Thus, by considering only feasible SoC trajectories, the j -th price threshold for the k -min algorithm defined as follows:

$$\ell_i^{\text{dis}}(t, e_t) = \frac{\omega}{K_{\min}^{\text{feas}}(t, e_t)} \left(\sum_{\hat{t}=1}^{t-1} \sum_{k=1}^{i-1} \ell_k^{\text{dis}}(\hat{t}) + \sum_{n=1}^{K_{\min}^{\text{feas}}(t, e_t)} z_n^{\min|\text{feas}}(t, e_t) \right),$$

where $K_{\min}^{\text{feas}}(t, e_t)$ is the maximum number of discharge actions that are feasible from the current SoC at t . Here,

$z_n^{\min|\text{feas}}(t, e_t)$ are the smallest predicted prices restricted to future time slots where the battery can actually discharge on at least one feasible trajectory. The same logic is used to compute the k-max thresholds ($u_i^{\text{ch}}(t, e_t)$) while restricting them to only feasible trajectories. Appendix C describes how $K^{\text{feas}}(t, e_t)$ is computed from the SoC bounds and rate limits, and how the feasibility-restricted predicted price sets $z_n^{\min|\text{feas}}(t, e_t)$ are constructed and used in the benchmark.

Battery assets can leverage forecast information, such as price bounds (dashed blue lines in Fig. 2), or distribution estimates to account for the price uncertainty. Given the predetermined price thresholds sequences $\{u_j(t)\}_{j=1}^{k_{\text{ch}}}$ and $\{\ell_i(t)\}_{i=1}^{k_{\text{dis}}}$, the asset can evaluate a price distribution $F(\boldsymbol{\lambda})$ and compute at each time t the probabilities of charging, discharging, or idling. We denote these probabilities as α_t , β_t , and γ_t , respectively, which are essential for evaluating feasibility of the chance constraint in (3d). For instance,

$$\alpha_t = \int F(\boldsymbol{\lambda}_t \geq u^{\text{ch}}(t)) d\boldsymbol{\lambda}_t, \quad (8a)$$

$$\beta_t = \int F(\boldsymbol{\lambda}_t \leq \ell^{\text{dis}}(t)) d\boldsymbol{\lambda}_t, \quad (8b)$$

$$\gamma_t = 1 - \alpha_t - \beta_t. \quad (8c)$$

The expressions in (8) give the time dependent probabilities of charging, discharging, and idling under $F(\boldsymbol{\lambda})$. Propagating these probabilities through the SoC constraint in (3b) yields the induced distribution of e_T , which allows us to evaluate the chance constraint in (3d).

B. Uncertainty quantification for the terminal state-of-charge
Under the threshold price policy described in Section II-A, we assume that the probability of taking action a_t can be measured by evaluating possible price distribution of $\boldsymbol{\lambda}_t$. The probabilities $\alpha_t, \beta_t, \gamma_t \geq 0$ from (8) satisfy $\alpha_t + \beta_t + \gamma_t = 1$, forming a valid distribution over the three mutually exclusive actions. Hence, the SoC value at T can be quantified by considering the terminal value $e_T = e_0 + \sum_{t=1}^T Y_t$, where $Y_t = a_t P$ is the net injection at T , which is defined as:

$$Y_t = \begin{cases} +P, & \text{with probability } \alpha_t, \\ 0, & \text{with probability } \gamma_t, \\ -P, & \text{with probability } \beta_t. \end{cases} \quad (9)$$

We are interested in computing $\mathbb{P}_{\boldsymbol{\lambda}}\{e_T \in \mathcal{E}\}$ and then in estimating the number of charging (r_{ch}) and discharging (r_{dis}) actions to compute e_T . Consider then, $r_{\text{ch}} = \sum_{t=1}^T \mathbb{1}(a_t = 1)$, $r_{\text{dis}} = \sum_{t=1}^T \mathbb{1}(a_t = -1)$, where $\mathbb{1}(\cdot)$ corresponds to an indicator function, equal to 1 when the condition inside the parentheses holds, and 0 otherwise. The terminal SoC satisfies $e_T = e_0 + P(r_{\text{ch}} - r_{\text{dis}})$. To characterize the trajectories that lead to the SoC target band, we express $e_T \in \mathcal{E}$ as bounds on the number of charging minus discharging actions, i.e. $\underline{S} \leq r_{\text{ch}} - r_{\text{dis}} \leq \bar{S}$ where \underline{S} and \bar{S} are defined as:

$$\underline{S} = \frac{e^{\text{target}} - \delta - e_0}{P}, \quad \bar{S} = \frac{e^{\text{target}} + \delta - e_0}{P}. \quad (10)$$

The probability of finishing within the SoC target band:

$$\mathbb{P}_{\boldsymbol{\lambda}}\{e_T \in \mathcal{E}\} = \mathbb{P}_{\boldsymbol{\lambda}}\{\underline{S} \leq r_{\text{ch}} - r_{\text{dis}} \leq \bar{S}\},$$

which could then be expressed using (8) and (10) as:

$$\mathbb{P}_{\boldsymbol{\lambda}}\{e_T \in \mathcal{E} \mid \kappa_{k_{\text{dis}}}^{k_{\text{ch}}}\} = \kappa_{k_{\text{dis}}}^{k_{\text{ch}}} \sum_{\Delta r} \sum_{A \subseteq \mathcal{T}} \sum_{B \subseteq \mathcal{T} \setminus A} \prod_{t \in A} \alpha_t \prod_{t \in B} \beta_t \prod_{t \notin A \cup B} \gamma_t, \quad (11a)$$

$$\underline{S} \leq \Delta r = r_{\text{ch}} - r_{\text{dis}} \leq \bar{S}, \quad |A| = r_{\text{ch}}, \quad |B| = r_{\text{dis}}, \quad (11b)$$

where $\kappa_{k_{\text{dis}}}^{k_{\text{ch}}}$ corresponds to the probability that the battery asset chooses specific k_{ch} and k_{dis} values, where the sum of κ is equal to 1. Here, $A = A(e_t, t) \subseteq \mathcal{T}$ is the subset of time indices in which the charging action occurs, $A(e_t, t) = \{t \in \mathcal{T} : \mathbb{1}(a_t = 1) = 1, E_{\min} \leq e_t \leq E_{\max} \forall t \leq T\}$ and $B = B(e_t, t) \subseteq \mathcal{T} \setminus A$ is the subset of time indices in which the discharging action occurs, $B(e_t, t) = \{t \in \mathcal{T} : \mathbb{1}(a_t = -1) = 1, E_{\min} \leq e_t \leq E_{\max} \forall t \leq T\}$. To explicitly evaluate feasible trajectories for the probability constraint (11), we employ a pruning and probability redistribution algorithm that forward-propagate and adjust the probability mass through feasible SoC transitions over the time horizon, reducing the size of the action/decision tree of the battery storage problem.

We assume that the battery asset adopts, as a pre-policy $\kappa_{k_{\text{dis}}}^{k_{\text{ch}}}$, a predefined pair $(k_{\text{ch}}, k_{\text{dis}})$ and then computes the expected profit based on the price thresholds and the evaluated price distribution. If the tuple $(k_{\text{ch}}, k_{\text{dis}})$ is not profitable, it is discarded. From the remaining combinations, the probability of selecting any one of them is equally distributed. Finally, if the remaining horizon or SoC state can no longer support the originally planned $(k_{\text{ch}}, k_{\text{dis}})$ actions given the realized price sequence $\boldsymbol{\lambda}$, these values are reduced to maintain feasibility over the remaining time, as described in Appendix A.

C. Pruning and probability redistribution algorithm

To compute the exact SoC distribution under operational constraints, and to avoid propagating probability mass through infeasible SoC trajectories, we propose a simple pruning approach, which we call *probability redistribution*. This algorithm is a deterministic, dynamic-programming-based adjustment that maintains a forward-propagated probability mass function $\text{dist}_t[e]$ for the SoC at each time t . At $t = 0$, we initialize $\text{dist}_0[e_0] = 1$. For each subsequent time step, we compute tentative transition probabilities α_t , β_t , and γ_t of charging, discharging, and idling, based on the price-threshold policy in (8). Given a value of SoC e_t , whenever an action would push the SoC outside the limits $[E_{\min}, E_{\max}]$, we fold its probability mass into the idle branch. This means that for each level e_t , the infeasible probability fraction α_t or β_t is added to γ_t , before set it to zero for that state and time. Propagating these adjusted probabilities from $t = 1$ to T yields an exact $\text{dist}_T[e]$, from which we can compute the probability of meeting the terminal band and the minimum stopping time (e.g. referred above as the *replanning point*). For example, in Fig. 3, the purple arrow path shows a possible path from τ to $\tau + 2$. In this state, charging is unfeasible (red arrow), so its related probability $\alpha_{\tau+2}$ is added to the idle (purple arrow) probability action $\gamma_{\tau+2}$ and set to zero for that state.

Fig. 4 shows a probability heat map for the SoC using the *probability redistribution* algorithm for $T = 6$. The battery limits are set $E_{\min} = 30$ MWh and $E_{\max} = 50$ MWh.

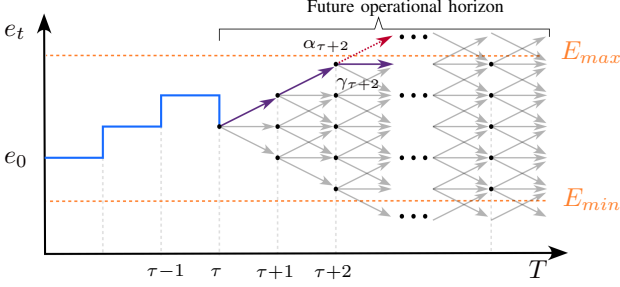


Fig. 3: Pruning and probability redistribution algorithm.

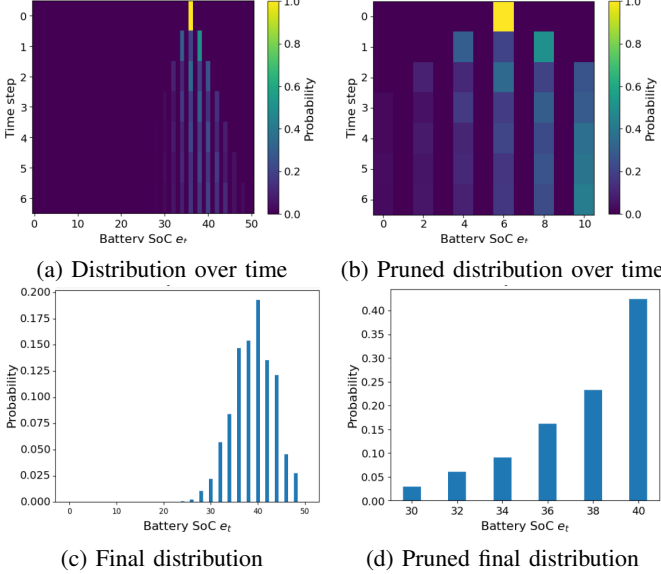


Fig. 4: (a) Non-pruning SoC distribution over time. (b) Pruning SoC distribution over time. (c) Non-pruning terminal SoC distribution. (d) Pruning terminal SoC distribution.

D. Stopping-time for the battery asset

In online decision problems, stopping time criteria arise from optimal-stopping theory and the analysis of competitive online algorithms (e.g., the secretary problem). A stopping time τ is a stopping time with respect to the observed price process if the decision to stop at t depends only on $\{\lambda_n\}_{n=1}^t$. The goal is to design τ^* so as to maximize a performance metric, in this case satisfy the chance constraint of staying within \mathcal{E} , without foreknowledge of future prices. Thus, the minimum stopping time in this problem looks for the latest period $\tau^* \leq T$ that guarantees $\mathbb{P}_\lambda\{e_T \in \mathcal{E}\}$ at level $(1-\epsilon)$ under a threshold policy and given the uncertain price sequence $\{\lambda_t\}_{t=1}^T$.

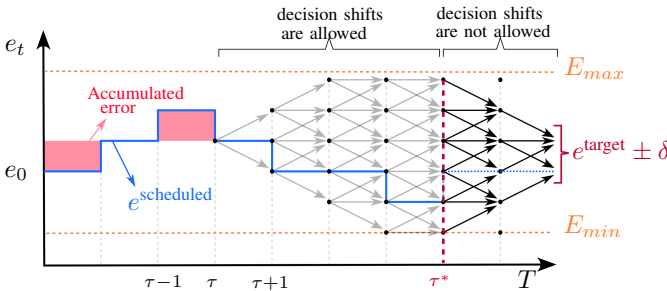


Fig. 5: Stopping-time for the battery arbitrage problem.

Fig. 5 shows an example of the battery storage problem,

where τ^* is the last period that guarantees the chance constraints can be satisfied, even with full control of the battery. Here, τ^* represents the minimum stopping-time in the RT market, relative to the DA schedule, at which the battery owner must begin conserving energy to ensure that the SoC finishes within the red target band \mathcal{E} at T . This conservative period balances the desire to exploit favorable RT prices against the risk of price-driven deviations from the DA plan, thereby safeguarding the probability of meeting the energy target band.

To compute the minimum stopping time, we first compute the probability transitions in (8), and then, apply the *probability redistribution* to construct $\forall t \in \mathcal{T}$ and all feasible e_t , the joint distribution $\mathbb{P}_\lambda\{e_t = e, e_T \in \mathcal{E}\}$. From this, we derive:

$$\text{dist}_t[e] = \mathbb{P}_\lambda\{e_t = e\}, \quad (12a)$$

$$q_t(e) = \mathbb{P}_\lambda\{e_T \in \mathcal{E} \mid e_t = e\}. \quad (12b)$$

Then, the overall probability Q_t of satisfying the terminal SoC band by time T , conditioned on stopping at t , is $Q_t = \sum_e \text{dist}_t[e] q_t(e)$. Taking this value, we can define the minimum stopping time as $\tau^* = \min\{t : Q_t \geq 1 - \epsilon\}$.

Thus, by declaring τ^* to the system operator and ceasing all charging and discharging actions thereafter, the operator can ensure, with confidence at least $(1-\epsilon)$, that the battery's SoC at time T will lie within \mathcal{E} . Declaring τ^* ahead of time gives the system operator advance notice of when the battery will cease market participation, which can be incorporated into reserve scheduling, critical-hour planning and other routines. Furthermore, by evaluating the stopping time in Section II-B, we can derive conservative threshold prices for battery actions that inform the pricing of the stopping action.

III. CONFORMALIZED QUANTILE REGRESSION FOR THE BATTERY ENERGY ARBITRAGE

To compare the probability estimates from Section II-A, we implemented *conformalized quantile regression* (CQR), which uses historical daily energy price samples and the corresponding end-of-horizon SoC under the threshold policy to construct a prediction set for the terminal SoC [34], [30].

We consider the daily energy price as i.i.d. samples. For each day n , let λ_n denote the input features (e.g., full daily price trajectory and the initial SoC e_0), and let $e_{T,n}$ denote the final SoC, which is the outcome of the threshold policy from Section II-A. We split the historical price series into a training set $\mathcal{D}_{\text{train}}$, a calibration set $\mathcal{D}_{\text{calib}}$, and a test set $\mathcal{D}_{\text{test}}$. Given a test price samples $\lambda^{\text{test}} = \{\lambda_n^{\text{test}}\}_{n \in \mathcal{D}_{\text{test}}}$, CQR builds a prediction set $\mathcal{C}(\lambda^{\text{test}})$ for the threshold policy outcome e_T^{test} .

The goal is to guarantee marginal coverage at level $1 - \epsilon$ across sample energy price sequences. Thus, the probability estimates and the prediction set could be expressed as follows:

$$\mathbb{P}_\lambda\{e_T^{\text{test}} \in \mathcal{C}(\lambda^{\text{test}})\} \geq 1 - \epsilon, \\ \mathcal{C}(\lambda^{\text{test}}) = \{e : S(\lambda^{\text{test}}, e) \leq \hat{q}\},$$

where $S(\cdot)$ is a nonconformity score and \hat{q} is an empirical quantile computed using the calibration data. In particular, the set $\mathcal{C}(\cdot)$ can be taken as a box (interval) set, so that $\mathcal{C}(\lambda) = [L(\lambda), U(\lambda)]$, which can be interpreted as a sample-based approximation built from historical pairs (λ, e_T) .

We first fit a quantile regression model for the conditional distribution $\{e_{T,n}|\lambda_n\}_{n=1}^N$, producing a lower conditional quantile \hat{q}_{low} and an upper quantile \hat{q}_{high} . On $\mathcal{D}_{\text{train}}$, we train a base quantile regression model at levels $\rho_{\text{low}} = \frac{\epsilon}{2}$ and $\rho_{\text{high}} = 1 - \frac{\epsilon}{2}$ to obtain $\hat{q}_{\text{low}}(x) \approx Q_{e_T|\lambda=x}(\rho_{\text{low}})$ and $\hat{q}_{\text{high}}(x) \approx Q_{e_T|\lambda=x}(\rho_{\text{high}})$ via pinball loss, i.e., $L_\theta(y, \hat{y}) = \max(\theta(y - \hat{y}), (\theta - 1)(y - \hat{y}))$ where θ is the target quantile.

For each $n \in \mathcal{D}_{\text{calib}}$, we check the realized price sequence with the threshold policy to obtain $e_{T,n}$, evaluate the predicted quantiles $\hat{q}_{\text{low}}(\lambda_n)$ and $\hat{q}_{\text{high}}(\lambda_n)$ and compute the nonconformity score $S_n = \max[\hat{q}_{\text{high}}(\lambda_n) - e_{T,n}, e_{T,n} - \hat{q}_{\text{low}}(\lambda_n), 0]$, where S_n could be interpreted as how far $e_{T,n}$ falls outside the predicted interval $[\hat{q}_{\text{low}}(\lambda_n), \hat{q}_{\text{high}}(\lambda_n)]$.

Let define $n_{\text{calib}} = |\mathcal{D}_{\text{calib}}|$ and $\gamma = \lceil (n_{\text{calib}}+1)(1-\epsilon) \rceil / n_{\text{calib}}$. We take the empirical γ -quantile of $\{S_n\}_{n \in \mathcal{D}_{\text{calib}}}$ and denote it by $\hat{\Delta}$. This value adjusts the model interval to correct miscoverage, where if the model is accurate $\hat{\Delta} \rightarrow 0$, otherwise $\hat{\Delta}$ will increase its value to correct mispredictions. Finally, for each test day $n \in \mathcal{D}_{\text{test}}$, we compute the conformalized bounds $\tilde{L}(\lambda_n) = \hat{q}_{\text{low}}(\lambda_n) - \hat{\Delta}$ and $\tilde{U}(\lambda_n) = \hat{q}_{\text{high}}(\lambda_n) + \hat{\Delta}$, and define the final conformalized prediction interval for $e_{T,n}$ as follows:

$$C(\lambda_n) = [\tilde{L}(\lambda_n), \tilde{U}(\lambda_n)] \quad (13)$$

Thus, $C(\lambda_n)$ provides a $(1-\epsilon)$ interval for the terminal SoC under the threshold policy and daily energy price sequences. In principle, if for a given day the conformal interval satisfies $C(\lambda_n) \subseteq \mathcal{E}$, then the terminal SoC e_T lies within the SoC target band with probability at least $(1-\epsilon)$ with respect to the CQR marginal coverage guarantee.

IV. CASE STUDY

In this section, we present computational experiments that compare the proposed framework from Section II-A and III using real-world PJM data. Section II-A defines the threshold policy and the stopping time requirement for the SoC outcomes under price uncertainty. We use the probability-redistribution procedure in Section II-B to estimate the probability of finishing within a SoC target band, and to study its sensitivity to the initial state and the time at which the battery operation initiated (hereafter *start time window*). We use the conformalized quantile regression (CQR) model from Section III to build prediction intervals for the terminal SoC and to assess out-of-sample coverage and target band certificates.

We use six years of real-world PJM data, $\{\lambda_i\}_{i=1}^N$, similarly to [35], and use the hourly energy prices as an input to the arbitrage policy and CQR model. The operation time horizon is $T = 24$, and the target set consists of the terminal hour only, i.e., $\mathcal{T}^{\text{target}} = \{24\}$. Battery limits are $E_{\min} = 0$ and $E_{\max} = 10$ MWh, with maximum charge and discharge rate $P = 2$ MW. In our simulation, we vary the initial SoC over $e_{t=0} \in \{1, \dots, 9\}$ MWh to show the sensibility of the resulting probabilities. We consider two terminal SoC target bands, $\mathcal{E} = [5, 7]$ MWh and $\mathcal{E} = [3, 8]$ MWh to evaluate how the terminal SoC probability changes under a stricter vs looser requirement. We evaluate multiple SoC values and start-time windows (e.g. running the algorithm from $t = 3$ instead $t = 0$). For each case, we estimate the probability of satisfying the SoC target band constraint in eq. (2) and quantify the associated profit

outcomes under the threshold policy.

To operationalize the the CQR model on the PJM data with price coverage level $(1-\epsilon) = 0.9$, we split the historical price series into 60% training data, 20% calibration data, and 20% test data. For each test day $n \in \mathcal{D}_{\text{test}}$, CQR returns a prediction interval $C(\lambda_n) = [\tilde{L}(\lambda_n), \tilde{U}(\lambda_n)]$ for the terminal SoC $e_{T,n}$ under the threshold policy. In addition to verifying the marginal coverage of $C(\lambda_n)$, we also compute how often $C(\lambda_n) \subseteq \mathcal{E} = [3, 8]$ MWh, since this inclusion certifies that $e_{T,n} \in \mathcal{E}$ with confidence at least $(1-\epsilon)$.

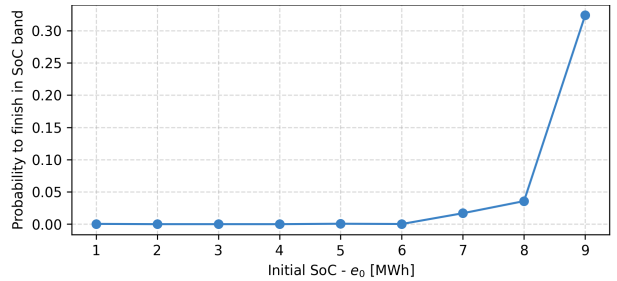


Fig. 6: Probability that the battery attains the SoC target band $\mathcal{E} = [5, 7]$ MWh, given a start time $t = 0$.

Fig. 6 shows that the probability that the battery finishes within a given SoC target band is highly sensitive to the initial SoC e_0 . Particularly, when e_0 is low, the probability of finishing within \mathcal{E} is close to zero, and it increases only when e_0 is already near the upper range of \mathcal{E} . This behavior is driven by the limited rate P , the finite number of actions over the horizon and, also, since the battery follows a policy that must have a positive expected profit, the set of feasible trajectories that lead to the target band is small if the initial e_0 starts far below \mathcal{E} . Fig. 7 shows the probability of reaching the SoC target band while varying the start time. Intuitively, initiating the policy later reduces the remaining flexibility to correct the SoC trajectory and limits the available arbitrage opportunities. When e_0 is already above \mathcal{E} , start later may reduce the number of trajectories that drift it outside the band. Thus, the probability to finish within the SoC target band depends on the state (through e_0) and time (through the start time and realized price sequence), which makes the stopping time τ^* difficult to satisfy across all values e_0 .

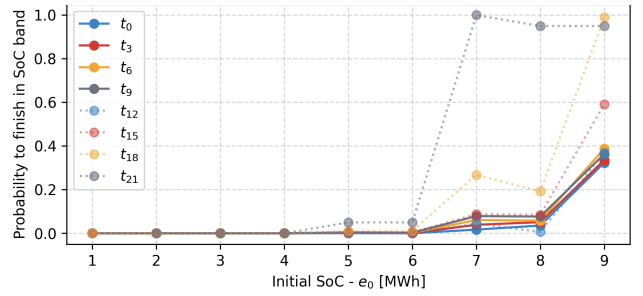


Fig. 7: Probability that the battery finishes within the SoC target band $\mathcal{E} = [5, 7]$ MWh, for different start time windows.

Table I shows the ratio between the number of SoC trajectories that leads to \mathcal{E} and the total number of feasible trajectories across different initial SoC values and start time windows (without considering the battery policy). The probability of

Initial SoC [MWh]	SoC band [MWh]	Start time hour			
		0	6	12	18
1	[5, 7]	46.66	43.63	37.14	20.00
	[3, 8]	73.17	72.97	71.43	60.00
5	[5, 7]	50.01	50.10	50.72	55.56
	[3, 8]	73.22	73.31	73.91	77.78
9	[5, 7]	53.29	55.98	60.00	60.00
	[3, 8]	73.17	72.97	71.43	60.00

TABLE I: Percentage of feasible trajectories that finish within the SoC target band \mathcal{E} , by initial SoC and start time windows.

reaching a tight terminal band $\mathcal{E} = [5, 7]$ MWh varies significantly with e_0 . For $e_0 \geq 3$ MWh, the probability generally increases with e_0 and the start time, whereas for $e_0 \leq 3$ it tends to decrease as the start time window shifts later. When the band is wider, $\mathcal{E} = [3, 8]$ MWh, overall probabilities increase, but for initial SoC values outside the target band, the probability tends to decrease with e_0 and with the start time window.

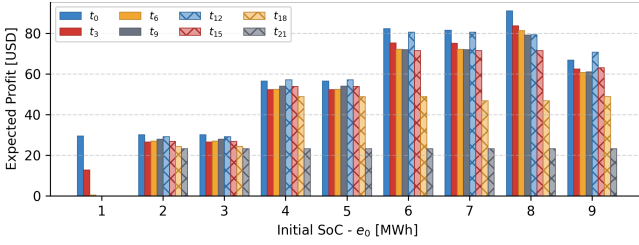


Fig. 8: Accumulated battery profit under the threshold policy for different start time windows.

Fig. 8 shows the accumulated battery profit under the threshold policy for different start time windows and initial SoC values. The profit outcomes vary across start time windows, since that intraday price differs depending on when the policy is initiated, and conservative actions taken to preserve feasibility can reduce the exploitation of arbitrage opportunities. Together with Fig. 7, these results highlight a SoC target reachability and profit trade-off. Dispatching the battery to increase the probability of finishing within \mathcal{E} can reduce the attainable arbitrage profit under the same realized price sequence.

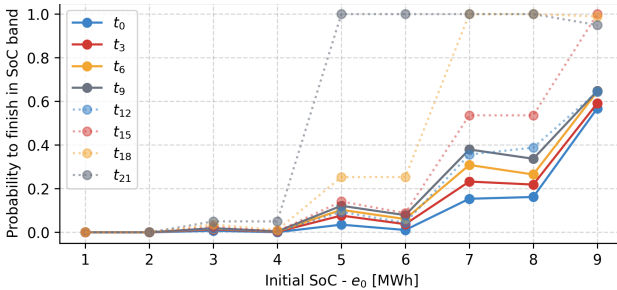


Fig. 9: Probability that the battery finishes within the SoC target band $\mathcal{E} = [3, 8]$ MWh, for different start time windows.

Fig. 9 shows that widening the terminal band increases the success probabilities across most initial SoC values and start time windows, as expected. However, the dependence on both e_0 and the start time remains, even under a wider terminal interval, the probability curves are not uniform across start time windows, indicating that time-of-day effects persist. The stopping time τ^* has a stronger dependence on e_0 . For

instance, when $e_0 \geq 5$ MWh, the choice $\tau^* = 21$ hr guarantees reachability of the SoC target band, whereas for $e_0 \leq 5$ MWh the associated probability decreases to below 0.2. Similarly, when $e_0 \geq 7$ MWh and $\tau^* = 15$ hr, the probability of reaching the band is approximately 0.55, but it drops to below 0.2 when $e_0 \leq 7$ MWh.

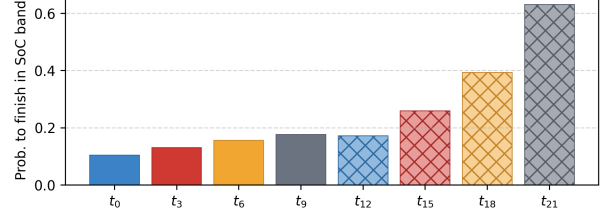


Fig. 10: Average probability that the battery finishes within the SoC target band $\mathcal{E} = [3, 8]$ between initial SoC.

Finally, Fig. 10 displays an aggregated comparison across start windows by averaging the probability of finishing within $\mathcal{E} = [3, 8]$ MWh across the initial SoC values. The results provide a simple insight into the overall increasing tendency in the probability of reaching the target band as the start window shifts later, suggesting that a stopping time τ^* without state dependency could not provide, for the proposed battery policy, guarantees above 60%.

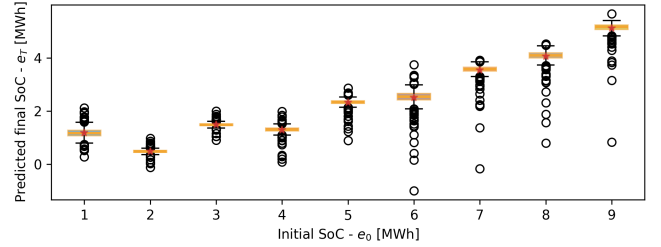


Fig. 11: Distribution of predicted terminal SoC e_T across test data for each initial SoC e_0 and price coverage $(1 - \epsilon) = 0.9$.

To complement the probability analysis above, we next use CQR to predict the terminal SoC using the historical PJM data varying the initial SoC e_0 . Fig. 11 shows the distribution of the predicted terminal SoC from the CQR model across test days for each initial SoC value e_0 , at price coverage level $(1 - \epsilon) = 0.9$. The black markers correspond to individual test-day predictions, while the orange markers summarize the 25th–75th percentile for each e_0 . As e_0 increases, the predicted terminal SoC tends to increase, and its dispersion also grows. This provides insight that terminal SoC e_T under the threshold policy is mainly driven by the initial SoC e_0 .

Fig. 12 shows how the out-of-sample guarantees vary with the initial SoC. The empirical price coverage remains close to one for most values of e_0 , indicating that the conformalized intervals preserve the desired marginal coverage for the terminal SoC induced by the threshold policy. In contrast, the SoC target band coverage, fraction of days which $C(\lambda) \subseteq \mathcal{E}$, is low for small e_0 and increases as e_0 approaches the SoC target. For example, when $e_0 > 7$ MWh the target band coverage reaches 0.7. Since the CQR does not enforce $C(\lambda) \subseteq \mathcal{E}$, this coverage gap is expected, i.e., no guarantee that the resulting interval lies entirely inside \mathcal{E} . Thus, the chance constraint in

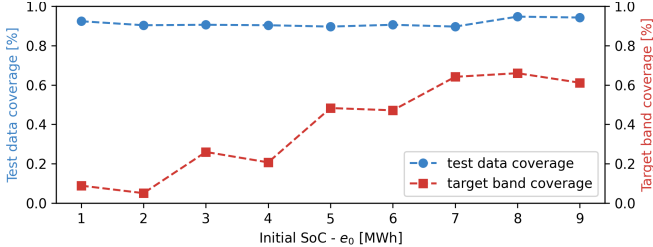


Fig. 12: Coverage versus the initial SoC. The blue curve shows the empirical test-set coverage (fraction of realizations for which $e_T \in C(\lambda)$). The red curve shows the SoC target band coverage between different e_0 (fraction of test days for which the predicted interval is contained in the SoC target band, $C(\lambda) \subseteq \mathcal{E}$). The price coverage $(1 - \epsilon) = 0.9$, and $\mathcal{E} = [3, 8]$.

(3d) is rarely satisfied for low e_0 and increases for larger e_0 values, because the policy is more likely to meet the fixed band \mathcal{E} , when the initial state is nearer to the prescribed band.

V. CONCLUSION AND FUTURE WORK

This paper presents a framework for battery energy arbitrage under uncertain energy prices that integrates an approximate chance-constrained terminal SoC requirement, defined by a safe SoC target band, with online threshold policies. Using a k -search structure, we derive explicit buy and sell thresholds, compute the induced action and terminal SoC probabilities over the planning horizon. To obtain exact SoC distributions under operational limits, we develop a probability redistribution pruning algorithm and use it to quantify the probability of staying within the SoC target band and to estimate the stopping time required to satisfy the SoC chance constraint.

Results on historical PJM data indicate that the terminal SoC is highly sensitive to the initial SoC (e_0) and the operation start time. When e_0 starts far from the terminal SoC target band, the limited charge/discharge rate and the finite operation horizon leave few feasible trajectories that can reach the SoC target band. Similarly, initiating the policy later (i.e., greater start time) reduces the remaining flexibility to correct the SoC trajectory and limits available arbitrage opportunities, yielding inconsistent success probabilities across start time windows. While widening the terminal band increases success probabilities, the dependence on both state and time persists, making a single state-independent stopping time τ^* difficult to satisfy across all cases. These results also highlight a reliability/profit trade-off, where increasing the probability of finishing within the SoC target band can reduce the attainable arbitrage profit under the same realized price sequence. In addition, CQR preserves the desired marginal out-of-sample coverage for the terminal SoC under the threshold policy, but does not yield prediction intervals contained within a prescribed SoC target band, which explains the observed gap between marginal and target band coverage for small e_0 values.

REFERENCES

- [1] D. Bienstock et al., “Risk-aware security-constrained unit commitment: Taming the curse of real-time volatility and consumer exposure,” *IEEE Trans. on Energy Markets, Policy and Regulation*, 2024.
- [2] CAISO, “2023 special report on battery storage,” tech. rep., 2024.
- [3] Department of Market Monitoring, “Comments on minimum state of charge extension: Straw proposal,” comments, CAISO, Feb. 2023.
- [4] PUCT, “1186NP36 PUCT Report 041124,” tech. rep., PUCT, 2024.
- [5] Y. M. Al-Abdullah, M. Abdi-Khorsand, and K. W. Hedman, “The role of out-of-market corrections in day-ahead scheduling,” *IEEE Trans. Power Syst.*, vol. 30, no. 4, pp. 1937–1946, 2014.
- [6] A. Ahmad et al., “Renewable integration and energy storage management and conversion in grid systems: A comprehensive review,” *Energy Reports*, vol. 13, pp. 2583–2602, 2025.
- [7] R. Sioshansi et al., “Energy-storage modeling: State-of-the-art and future research directions,” *IEEE Trans. Power Syst.*, vol. 37, no. 2, 2021.
- [8] R. Sioshansi, P. Denholm, T. Jenkin, and J. Weiss, “Estimating the value of electricity storage in pjm: Arbitrage and some welfare effects,” *Energy economics*, vol. 31, no. 2, pp. 269–277, 2009.
- [9] D. McConnell et al., “Estimating the value of electricity storage in an energy-only wholesale market,” *Applied Energy*, vol. 159, 2015.
- [10] B. Xu et al., “Operational valuation of energy storage under multi-stage price uncertainties,” in *2020 59th IEEE CDC*, pp. 55–60, IEEE, 2020.
- [11] Y. Dvorkin et al., “Ensuring profitability of energy storage,” *IEEE Trans. Power Syst.*, vol. 32, no. 1, pp. 611–623, 2016.
- [12] X. Zhang et al., “Arbitrage analysis for different energy storage technologies and strategies,” *Energy Reports*, vol. 7, pp. 8198–8206, 2021.
- [13] N. G. Singhal and E. G. Ela, “Pricing impacts of state of charge management options for electric storage resources,” in *2020 IEEE Power & Energy Society General Meeting (PESGM)*, pp. 1–6, IEEE, 2020.
- [14] D. Krishnamurthy et al., “Energy storage arbitrage under day-ahead and real-time price uncertainty,” *IEEE Trans. Power Syst.*, vol. 33, no. 1, pp. 84–93, 2017.
- [15] N. Zheng, J. Jaworski, and B. Xu, “Arbitraging variable efficiency energy storage using analytical stochastic dynamic programming,” *IEEE Trans. Power Syst.*, vol. 37, no. 6, pp. 4785–4795, 2022.
- [16] Y. Chen and R. Baldick, “Battery storage formulation and impact on day ahead security constrained unit commitment,” *IEEE Trans. Power Syst.*, vol. 37, no. 5, pp. 3995–4005, 2022.
- [17] N. Qi et al., “Chance-constrained generic energy storage operations under decision-dependent uncertainty,” *IEEE Trans. Sust. Ener.*, vol. 14, no. 4, pp. 2234–2248, 2023.
- [18] N. Qi et al., “Chance-constrained energy storage pricing for social welfare maximization,” *arXiv preprint arXiv:2407.07068*, 2024.
- [19] M. Zhang et al., “Day-ahead optimization dispatch strategy for large-scale battery energy storage considering multiple regulation and prediction failures,” *Energy*, vol. 270, p. 126945, 2023.
- [20] B. Cheng and W. Powell, “Co-optimizing battery storage for the frequency regulation and energy arbitrage using multi-scale dynamic programming,” *IEEE Trans. Smart Grid*, vol. 9, no. 3, 2016.
- [21] M. Babaioff et al., “Online auctions and generalized secretary problems,” *ACM SIGecom Exchanges*, vol. 7, no. 2, pp. 1–11, 2008.
- [22] M. H. DeGroot, “Some problems of optimal stopping,” *Journal of the Royal Stat. Soc. Series B: Stat. Meth.*, vol. 30, no. 1, pp. 108–122, 1968.
- [23] A. Pichler et al., “Risk-averse stochastic programming: Time consistency and optimal stopping,” *Operations Research*, vol. 70, no. 4, 2022.
- [24] J. Lorenz et al., “Optimal algorithms for k -search with application in option pricing,” *Algorithmica*, vol. 55, no. 2, pp. 311–328, 2009.
- [25] L. Yang et al., “Online linear optimization with inventory management constraints,” *Proc. ACM on Meas. and Analysis of Comp. Syst.*, vol. 4, no. 1, pp. 1–29, 2020.
- [26] R. Lee et al., “Online search with predictions: Pareto-optimal algorithm and its applications in energy markets,” in *Proc. of the 15th ACM Int. Conf. on Future and Sust. Ener. Syst.*, pp. 386–407, 2024.
- [27] L. Sang et al., “Electricity price prediction for energy storage system arbitrage: A decision-focused approach,” *IEEE Trans. Smart Grid*, vol. 13, no. 4, 2022.
- [28] A. Lechowicz et al., “The online pause and resume problem: Optimal algorithms and an application to carbon-aware load shifting,” *Proc. ACM on Meas. and Analysis of Comp. Syst.*, vol. 7, no. 3, pp. 1–32, 2023.
- [29] Y. Li, G. Qu, and N. Li, “Online optimization with predictions and switching costs: Fast algorithms and the fundamental limit,” *IEEE Trans. Automatic Control*, vol. 66, no. 10, pp. 4761–4768, 2020.
- [30] C. Yeh et al., “End-to-end conformal calibration for optimization under uncertainty,” *arXiv preprint arXiv:2409.20534*, 2024.
- [31] Y. Wu, M. Yi, B. Xu, and J. Anderson, “Online energy storage arbitrage under imperfect predictions: A conformal risk-aware approach,” *arXiv preprint arXiv:2511.01032*, 2025.
- [32] T. Tapia et al., “Learning reachability of energy storage arbitrage,” *arXiv preprint arXiv:2512.06600*, 2025.
- [33] B. Sun et al., “Competitive algorithms for the online multiple knapsack problem with application to electric vehicle charging,” *Proc. ACM on Meas. and Analysis of Comp. Syst.*, vol. 4, no. 3, pp. 1–32, 2020.

[34] Y. Romano, E. Patterson, and E. Candes, “Conformalized quantile regression,” *Advances in neural inf. processing syst.*, vol. 32, 2019.
[35] P. Dotti et al., “Task-based end-to-end model learning in stochastic optimization,” *Adv. neu. inf. proc. syst.*, vol. 30, 2017.

APPENDIX A

THRESHOLD POLICY COMPETITIVE GUARANTEE

Appendix is organized in three parts. First, we outline how the time-dependent thresholds competitive guarantee can be preserved when the effective k value is reduced mid-horizon by enforcing the same structural change on the benchmark. Second, we discuss how the feasibility constraints induced by the SoC capacity limits modify the set of admissible charge and discharge actions, and how this leads to a feasibility-dependent predicted price sets and thresholds.

A. Competitive guarantee proof for time-dependent thresholds

We present the proof for the discharge policy. The same arguments can be extended to the charge action. We consider the following time-dependent discharge threshold rule:

$$\ell_i^{\text{dis}}(t) = \frac{\omega}{k_{\text{dis}}} \left(\sum_{\hat{t}=1}^{t-1} \sum_{n=1}^{i-1} \ell_n^{\text{dis}*}(\hat{t}) + \sum_{m=1}^{k_{\text{dis}}-(i-1)} \hat{z}_m^{\min}(t) \right), \quad (14)$$

where ω is the target competitive ratio and $\hat{z}_m^{\min}(t)$ is the m -th smallest predicted price among future times. Intuitively, when no prediction is available the set $\hat{z}_m^{\min}(t) = \lambda^{\min}$ for all m and t . In this case, the term inside parentheses upper bounds the offline benchmark for the remaining discharge decisions. We denote it the offline benchmark $\text{OPT}_v^i(t)$ that satisfies:

$$\text{OPT}_v^i(t) \leq \left(\sum_{\hat{t}=1}^{t-1} \sum_{n=1}^{i-1} \ell_n^{\text{dis}*}(\hat{t}) + \sum_{m=1}^{k_{\text{dis}}-(i-1)} \hat{z}_m^{\min}(t) \right). \quad (15)$$

By construction, (14) guarantees the competitive bound by enforcing the following constraint:

$$\ell_i^{\text{dis}}(t) = \frac{\omega}{k_{\text{dis}}} \text{OPT}_v^i(t). \quad (16)$$

B. Mid-horizon reduction of k for policy decision

Let $G^{(k)}$ be the threshold outcome of the optimal k -max algorithm, $\text{OPT}^{(k)}$ be the offline optimum constrained to discharge k units, and $R(\cdot)$ be the associated reward as a function of the price sequence. The standard ω -competitive guarantee, where ω denotes the competitive ratio, can be expressed for any price sequence $p_{(1:T)} = \{p_t\}_{t=1}^T$ as follows:

$$R(G^{(k)}, p_{(1:T)}) \geq \frac{1}{\omega} \text{OPT}^{(k)}(T). \quad (17)$$

Suppose that at time $\bar{t}-1$ the policy has activated s discharge actions, and the remaining objective is reduced from k to $\bar{k} < k$ for $t \geq \bar{t}$. Over the remaining periods $[\bar{t}, T]$, the policy is required to discharge $k_{\text{rem}} = \bar{k} - s$ units. Let $G^{(k_{\text{rem}})}$ be the optimal k -search algorithm for the remaining periods, with its own reservation prices on the sub-horizon $p_{(\bar{t}:T)}$. Under this change, the original bound in (17) does not apply directly if the benchmark remains $\text{OPT}^{(k)}$, because the online and offline problems no longer share the same structure after \bar{t} .

To preserve a competitive statement, we define a modified benchmark $\overline{\text{OPT}}$ that aligns with structural change as the

online policy. We decompose the horizon into two stages. *Stage 1* that consider the range $[1, \bar{t}-1]$, where the benchmark $\overline{\text{OPT}}$ matches the online decisions by definition, and *Stage 2* over $[\bar{t}, T]$, where the benchmark is the offline optimum for the reduced subproblem of discharging k_{rem} . Thus, consider R_{stage1} and R_{stage2} as the online revenues in each of the previously defined stages, in particular, $R_{\text{stage1}}^{\text{bench}}$ and $R_{\text{stage2}}^{\text{bench}}$ are the rewards for the benchmark $\overline{\text{OPT}}$. By construction, $R_{\text{stage1}}^{\text{bench}} = R_{\text{stage1}}$. At Stage 2, the online policy runs the threshold policy $G^{(k_{\text{rem}})}$ on the remaining price sequence $p_{(\bar{t}:T)}$. Then, the reward on this stage corresponds to:

$$R_{\text{stage2}} = R(G^{(k_{\text{rem}})}, p_{(\bar{t}:T)}) \geq \frac{1}{\omega} \overline{\text{OPT}}^{(k_{\text{rem}})} = \frac{1}{\omega} R_{\text{stage2}}^{\text{bench}}. \quad (18)$$

Finally, define the total revenues $R^G = R_{\text{stage1}} + R_{\text{stage2}}$ and $R^{\text{bench}} = R_{\text{stage1}}^{\text{bench}} + R_{\text{stage2}}^{\text{bench}}$. Using (18), R^G satisfies:

$$\begin{aligned} R^G &\geq R_{\text{stage1}} + \frac{1}{\omega} R_{\text{stage2}}^{\text{bench}} = \frac{1}{\omega} (\alpha R_{\text{stage1}} + R_{\text{stage2}}^{\text{bench}}), \\ &\geq \frac{1}{\omega} (R_{\text{stage1}}^{\text{bench}} + R_{\text{stage2}}^{\text{bench}}) = \frac{1}{\omega} R^{\text{bench}}. \end{aligned} \quad (19)$$

Reducing k to k_{rem} preserves the competitive guarantee as long as the benchmark is also forced to share the same two-stage structure and pre-change actions. Then, for price sequence $p_{(1:T)}$ and two-stage structure, $R^G \geq \frac{1}{\omega} \overline{\text{OPT}}$.

C. Feasibility-aware thresholds and pruned action sets

Considering that the SoC constraints restrict the number of discharge (and charge) actions that can be executed from a given state (t, e_t) . In particular, the maximum number of feasible discharge actions from (t, e_t) is restricted as $K_{\text{max}}^{\text{dis}}(t, e_t) = \lfloor \frac{e_t - E_{\min}}{P} \rfloor$. This motivates us to replace the predicted-price set used in (8a) and (14) with a feasibility-aware version. We replace the predicted-price set as follows:

$$\{\hat{z}_m^{\min}(t)\}_{m=1}^{k_{\text{dis}}-(i-1)} \longrightarrow \{\hat{z}_m^{\min, \text{feas}}(t, e_t)\}_{m=1}^{K_{\text{rem}}(t, e_t)}, \quad (20)$$

where $K_{\text{rem}}(t, e_t) \leq K_{\text{max}}^{\text{dis}}(t, e_t)$ is the maximum number of remaining discharges that are feasible from the current state e_t , and $\hat{z}_m^{\min, \text{feas}}(t, e_t)$ is the m -th smallest predicted price restricted to time slots that can host at least one feasible discharge along some feasible path. Under this modification, the feasibility-aware discharge threshold becomes:

$$\ell_i^{\text{dis}}(t, e_t) = \frac{\omega}{K_{\text{rem}}(t, e_t)} \left(\sum_{\hat{t}=1}^{t-1} \sum_{n=1}^{i-1} \ell_n^{\text{dis}*}(\hat{t}) + \sum_{m=1}^{K_{\text{rem}}(t, e_t)} \hat{z}_m^{\min, \text{feas}}(t, e_t) \right). \quad (21)$$

Thus, we can define the feasibility-aware benchmark OPT_f at state (t, e_t) as follows:

$$\text{OPT}_f(t, e_t) = \left(\sum_{\hat{t}=1}^{t-1} \sum_{n=1}^{i-1} \ell_n^{\text{dis}*}(\hat{t}) + \sum_{m=1}^{K_{\text{rem}}(t, e_t)} \hat{z}_m^{\min, \text{feas}}(t, e_t) \right). \quad (22)$$

By construction, the threshold in (21) can be written compactly and enforcing to guarantee the competitive bound as:

$$\ell_i^{\text{dis}}(t, e_t) = \frac{\omega}{K_{\text{rem}}(t, e_t)} \text{OPT}_f(t, e_t). \quad (23)$$

This construction preserves the same scaling logic as in (16), but now enforces feasibility at the state level.